Bull. Chem. Soc. Jpn., 69, 853—860 (1996)

Attractive Potential Effect on the Rotational Correlation Times for Benzene-d_6 in Organic Solvents

Chihiro Wakai and Masaru Nakahara*

Institute for Chemical Research, Kyoto University, Uji, Kyoto 611

(Received December 7, 1995)

^{2}H NMR spin-lattice relaxation times have been measured to obtain the rotational correlation times τ_{2R} for benzene C_6D_6 (50 mol m^{-3}) in various organic solvents, such as benzene (C_6H_6), hexane, decane, carbon tetrachloride, chloroform, dichloromethane, methanol, ethanol, 1-propanol, 1-butanol, and acetonitrile over the widest possible range of temperature. Plots of the determined values of τ_{2R} against solvent viscosity η divided by temperature T are linear in the apolar and polar aprotic solvents, as predicted by the Stokes–Einstein–Debye (SED) law. However, the plots of τ_{2R} vs. η/T in the alcohols are concave upward, the slope in the high temperature region being ca. 2 times as large as that in the low temperature region. The nonlinearity and the decrease in the slope reflect the influence of the hydrogen-bonded solvent structure. For the benzene rotation in solutions, fairly good positive linear correlations are found between the slopes and the negative dissolution enthalpies at infinite dilution at room temperature. These results indicate an important role played by attractive solute–solvent interactions in controlling the molecular rotation in solution.

NMR spectroscopic studies can reveal a wealth of information about the rotational and translational mobilities $1/\zeta$ or friction coefficients ζ for constituent molecules in liquids. Such knowledge is needed for an understanding of fast photochemical reaction dynamics in solution at the Brownian motion level.[1] In the past decades, however, most dynamic NMR investigations have been confined to neat liquids or concentrated solutions with a linkage to the fundamental study of rate processes in solution.[2—4] The recent advance in NMR techniques has enabled us to measure very dilute solutions over a wide range of temperature and pressure in relation to solvation dynamics in the ground state.[5—12] The purpose of this paper is to clarify how the NMR correlation time τ_{2R} or the corresponding friction coefficient ζ_R for molecular rotation in solution is affected by the kinetic (collisional) and intermolecular attractive and repulsive potential factors involved in the time correlation function through the Hamiltonian. Only the repulsive solute–solvent interactions are taken into account on the macroscopic level, through the exclusion volume effect in the classical hydrodynamic model on which the Stokes–Einstein–Debye (SED) law is based. To encourage the development of a useful molecular theory for rotation of apolar molecules in dense liquid solutions, we want to accumulate experimental evidence for the necessity of considering the attractive intermolecular interactions as well as the repulsive ones. The rotational dynamics of such a symmetric molecule as benzene can be probed by the NMR method, but not by the dielectric one.

There are some practical reasons why we still rely upon the classical hydrodynamic law based on the continuum model. This primitive model neglects all the details of solute–solvent interactions and solvation structure in the short range; the molecular aspects are squeezed into the cavity or sphere boundary conditions for the solution to the Navier–Stokes equation of motion. The continuum mechanical approach coupled with the diffusion equations provides us simple analytical expressions for solution transport properties with an input of only a few solute and solvent parameters.[13] They are popular simply because the accessible rotational (SED) and translational (SE) transport properties for neat liquids can be converted into those necessary for the kinetic analysis of solutions of interest only in terms of solute size and bulk solvent viscosity, without the direct measurement.

The conventional hydrodynamic approach is however to be scrutinized before its application to an analysis of reaction dynamics in solution. Thus, it is nontrivial to test the validity for the apolar molecule of the SED law expressed by

$$\tau_{2R} = A\frac{\eta}{T}, \tag{1}$$

where η is the solvent viscosity, T is the temperature, and A is the hydrodynamic parameter characteristic of the solute size and the boundary conditions. For a hard spherical solute that interacts with the solvent via stick boundary conditions, the slope parameter for the isotropic rotation (IR), denoted by $A_{\mathrm{ST}}^{\mathrm{IR}}$, is expressed by

$$A_{\mathrm{ST}}^{\mathrm{IR}} = \frac{4\pi R^3}{3k_{\mathrm{B}}} \tag{2}$$

$$= \frac{V_{\mathrm{m}}}{k_{\mathrm{B}}}, \tag{3}$$

where k_{B} is the Boltzmann constant, and R and V_{m} are respectively the radius and the molecular volume of the solute. For a hard prolate or oblate ellipsoid with slip boundary conditions, a smaller parameter is used, depending on the shape factor.[14)] When the solute species is fixed as in this work, Eq. 2 predicts that the slope parameter is independent of solvent. Apart from the original meaning of the SED law, however, we can empirically regard the parameter as a measure of the effective volume that reflects the strength of solute–solvent interactions as well as the exclusion volume of the solute.[6,7)]

Our question is when and why Eq. 1 breaks down. To answer this, we need to carry out systematic experiments by selectively varying solute or solvent, temperature, and pressure. One may expect that the SED law is applicable to typical regular solutions formed by benzene with toluene, carbon tetrachloride, and cyclohexane, in which component dissimilarity in interaction is relatively weak. We have first derived a dynamical regular solution theory on the basis of the linear response and first-order perturbation theories, and then examined the applicability of the SED law for the interpretation of the concentration effect on the rotations of benzene (more precisely, of the C–D bonds) and solution viscosities in the typical regular solutions which are formed by the thermodynamically similar liquids.[15)] Notably, the relation between $\tau_{2\mathrm{R}}$ and η/T has been found not to be linear in benzene–cyclohexane, which is the most endothermic regular solution investigated.

In the present work, we extend this fundamental test with respect to solvent and temperature effects using a variety of organic solvents including protic and aprotic dipolar ones that yield strongly irregular solutions with benzene. To confirm a key role played by solute–solvent intermolecular interaction potentials in determining molecular rotation, here we scrutinize whether the effective hydrodynamic volume parameters for benzene in the organic solvents studied are correlated with the endothermic and exothermic dissolution enthalpies at infinite dilution available in the literature.[16)]

For a test of the continuum model, the rotational mode is preferable to the translational one because of the short range nature of rotation.[6,17)] In our previous studies,[5—7)] we have done comprehensive experiments on water molecules in apolar and polar organic solvents to test the SED law and the modified forms. The $\tau_{2\mathrm{R}}$ values for solitary water molecules do not follow Eq. 1, but exhibit somehow inverse proportionality to the solvent viscosity. This may be characteristic of water molecules which are: (i) unusually small in size, moment of inertia, and mass, and (ii) able to form strong and directional hydrogen bonds with proton donors and acceptors. The former and the latter are respectively associated with the kinetic and attractive potential factors influencing the rotational time correlation functions. The solute studied in the present work is uncharged, apolar, and larger in size, so that one may expect a more successful applicability of the SED law extended as mentioned above.

In the previous studies on ionic rotation in solution,[18,19)] we have focused on the dielectric friction theory where the dynamical attractive solute–solvent interactions are incorporated through the Coulomb- or Born-type expression within the continuum framework.[20,21)] Here we are concerned with neutral and apolar solute benzene. Its rotational motions are expected to be influenced not by the long-ranged dielectric frictional torques but more locally by such site–site interactions as dipole-induced dipole and hydrogen-bonding ones. Recent theoretical efforts are directed to develop the harmonic mode kinetic theory for hard particle fluids mimicking soft particle fluids to reproduce the SED behavior.[22)] This also motivates the present study on the apolar solute.

Theoretical

A reliable interpretation of the NMR relaxation data requires a proper understanding of the theoretical aspects and physical meaning of the magnetic relaxation, the spectral density, the rotational correlation time, the relevant friction coefficient, and so on. First, we introduce the essential theoretical backgrounds of the quadrupole relaxation for a symmetric top like benzene in solution.[23,24)] Second, we compute the slope value A in Eq. 1 on the basis of the classical hydrodynamics together with the rotational diffusion equation.

Correlation Time $\tau_{2\mathrm{R}}$ for the Symmetric Top. For the nuclear spin $I \geq 1$, the magnetic relaxation mechanism is dominated by the fluctuating interactions between an electric nuclear quadrupole moment (eQ) and the electric field gradient (EFG) at the nuclear site; e is the protonic charge. The mechanism is exclusively intramolecular and related to molecular rotation. In this case, we can ignore such other mechanisms as the dipole–dipole, chemical shift anisotropy, spin-rotation, and scalar coupling.

In the NMR relaxation study, the relatively small magnetic moment together with the central limit theorem allows us to treat a single spin instead of the macroscopic magnetization observed. The longitudinal (spin-lattice) relaxation of the z-component of the macroscopic magnetization is related to the ensemble-averaged behavior of a single spin whose z-component is I_z; the z axis of our laboratory-fixed frame is defined by the vertically applied static magnetic field. The quantum mechanical expression for the time evolution of the ensemble-averaged spin $\langle I_z \rangle$ is given as follows:

$$\frac{\mathrm{d}\langle I_z\rangle}{\mathrm{d}t} = -3\left\{\frac{2\pi eQ}{2I(2I-1)h}\right\}^2 \Big\{ j(\omega_0)\langle 16I_z{}^3 - 8I(I+1)I_z + 2I_z\rangle + j(2\omega_0)\langle -16I_z{}^3 + 16I(I+1)I_z - 8I_z\rangle \Big\}, \tag{4}$$

where

$$\langle I_z\rangle = \mathrm{tr}(\rho I_z), \tag{5}$$

$$j(\omega)=\frac{1}{2}\int_{-\infty}^{\infty}\langle F^{*}(0)F(t)\rangle\exp(-i\omega t)\mathrm{d}t. \qquad (6)$$

Here, h is the Planck constant, $j(\omega)$ is the spectral density at the frequency ω, ω_0 is the Larmor frequency, ρ is the density operator, $\langle F^{*}(0)F(t)\rangle$ is the ensemble average of the time correlation function representing the orientational decay, and the other symbols have the usual meaning.

For the case of deuterons (I=1), it holds that $I_z{}^3=I_z$. Hence Eq. 4 is simplified as

$$\frac{d\langle I_z\rangle}{\mathrm{d}t}=-\frac{1}{T_1}\langle I_z\rangle, \qquad (7)$$

where

$$\frac{1}{T_1}=\frac{6\pi^2}{5}\frac{2I+3}{I^2(2I-1)}\left(\frac{eQ}{h}\right)^2\{j(\omega_0)+4j(2\omega_0)\}. \qquad (8)$$

The spectral density function involved in the above equation takes an explicit form only when an analytically soluble model is introduced for the random orientational motion. For an axially symmetric molecule, the inertial theory based on the Langevin equation[24] yields the following expression:

$$j(\omega)=\left(1+\frac{1}{3}\xi^2\right)\frac{(eq)^2}{80}\left\{\frac{(3\cos^2\alpha-1)^2D_{\perp}\left(1+\dfrac{6I_{\perp}D_{\perp}}{\zeta_{\perp}}\right)}{36D_{\perp}^2+\omega^2}\right.$$
$$+\frac{\sin^2\alpha\cos^2\alpha(5D_{\perp}+D_{\|})\left(1+\dfrac{5I_{\perp}D_{\perp}}{\zeta_{\perp}}+\dfrac{I_{\|}D_{\|}}{\zeta_{\|}}\right)}{(5D_{\perp}+D_{\|})^2+\omega^2}$$
$$\left.+\frac{\sin^4\alpha(D_{\perp}+2D_{\|})\left(1+\dfrac{2I_{\perp}D_{\perp}}{\zeta_{\perp}}+\dfrac{4I_{\|}D_{\|}}{\zeta_{\|}}\right)}{(2D_{\perp}+4D_{\|})^2+\omega^2}\right\}. \qquad (9)$$

Here ξ is the asymmetric factor of EFG in the plain perpendicular to the direction of the largest principal EFG denoted by eq, α is the angle between the molecular symmetry axis (C_6) and the direction of q along the C–D bond, and D_i, ζ_i, and I_i are respectively the i-components of the rotational diffusion, the friction coefficient, and the moment of inertia; $\perp$ and $\|$ indicate the molecular rotations perpendicular and parallel to the symmetry axis, respectively. The rotational diffusion coefficient D_i and the rotational friction coefficient ζ_i are related by

$$D_i=k_{\mathrm{B}}T/\zeta_i, \qquad (10)$$

where the subscript "R" for rotation is abbreviated for simplicity.

In the Debye diffusion limit (I's→0), the inertial terms in the last factor in the numerator of each term in the curl brackets on the right-hand side of Eq. 9 drop; a Lorentzian function recovers from each term. Moreover, the extreme narrowing conditions are satisfied in usual solvents where molecular rotations are much faster than the resonance frequency ω. This approximation removes the frequency dependence of the spectral densities; that is to say,

$$j(0)=j(\omega)=j(2\omega). \qquad (11)$$

Combining Eqs. 8, 9, and 11 and neglecting the asymmetric factor, for I=1, we have

$$\frac{1}{T_1}=6\pi^2\frac{2I+3}{I^2(2I-1)}\left(\frac{eQ}{h}\right)^2 j(0) \qquad (12)$$

$$=\frac{9\pi^2}{4}\left(\frac{e^2Qq}{h}\right)^2\left\{\frac{(3\cos^2\alpha-1)^2}{36D_{\perp}}+\frac{\sin^2\alpha\cos^2\alpha}{5D_{\perp}+D_{\|}}+\frac{\sin^4\alpha}{4D_{\perp}+8D_{\|}}\right\}. \qquad (13)$$

This is to be compared with the usual expression for the quadrupole spin-lattice relaxation rate for I=1 given by

$$\frac{1}{T_1}=\frac{3\pi^2}{2}\left(\frac{e^2Qq}{h}\right)^2\tau_{2\mathrm{R}}. \qquad (14)$$

Here, the parenthesized quantity is the quadrupole coupling constant (QCC) for the ^{2}H nucleus, and the rotational correlation time for the C–D bond, which is to be denoted by $\tau_{2\mathrm{R}}$(C–D), is presented simply by $\tau_{2\mathrm{R}}$. From Eqs. 12, 13, and 14, we have

$$\tau_{2\mathrm{R}}=\frac{20}{(eq)^2}j(0) \qquad (15)$$

$$=\frac{3}{2}\left\{\frac{(3\cos^2\alpha-1)^2}{36D_{\perp}}+\frac{\sin^2\alpha\cos^2\alpha}{5D_{\perp}+D_{\|}}+\frac{\sin^4\alpha}{4D_{\perp}+8D_{\|}}\right\}. \qquad (16)$$

In the case of benzene-d_6, the angle α between the molecular symmetry axis and the direction of the C–D bond is $\pi/2$, so we have

$$\tau_{2\mathrm{R}}=\frac{3}{8}\left(\frac{1}{9D_{\perp}}+\frac{1}{D_{\perp}+2D_{\|}}\right). \qquad (17)$$

For the isotropic rotation, Eq. 17 is reduced to

$$\tau_{2\mathrm{R}}^{\mathrm{IR}}=\frac{1}{6D_{\perp}}=\frac{1}{6D_{\|}}=\frac{1}{6D^{\mathrm{IR}}}, \qquad (18)$$

where the superscript "IR" indicates isotropic rotation. Introduce a parameter χ to gauge the rotational anisotropy as

$$\chi=\frac{D_{\|}}{D_{\perp}}. \qquad (19)$$

With the help of the definitions by Eqs. 18 and 19, we can rewrite Eq. 17 as

$$\tau_{2\mathrm{R}}=f\tau_{2\mathrm{R}}^{\mathrm{IR}}, \qquad (20)$$

where

$$f=\frac{1}{4}\left(1+\frac{9}{1+2\chi}\right). \qquad (21)$$

It is to be noted that the f value is lower and upper bounded as

$$0.25<f<2.5. \qquad (22)$$

The lower and upper bounds may be provided by infinitely thin oblate (χ=∞) and long prolate tops (χ=0), respectively. The two extreme cases are associated with the slip boundary conditions.

Slope of the Relation between τ_{2R} and η/T. A hydrodynamic model[25)] may be applied for a symmetric top to evaluate χ. Under stick boundary conditions, we have

$$\frac{D_{\parallel}}{D_{\perp}}=\frac{\zeta_{\perp}}{\zeta_{\parallel}} \tag{23}$$

$$=\frac{b^2}{a^2+b^2}\left\{\frac{(2a^2-b^2)S-2a}{2a-b^2S}\right\}, \tag{24}$$

where

$$S=\frac{2}{(b^2-a^2)^{1/2}}\tan^{-1}\left\{\frac{(b^2-a^2)^{1/2}}{a}\right\},\quad b>a. \tag{25}$$

Here, a and b are the lengths of the shorter and longer axes, respectively, and for benzene,

$$a=0.170\ \text{nm},\quad b=0.360\ \text{nm}. \tag{26}$$

From Eqs. 19, 23, 24, 25, and 26 it follows that

$$\chi=\frac{\zeta_{\perp}}{\zeta_{\parallel}}=\frac{8.08}{6.46}=1.25. \tag{27}$$

Insertion of this anisotropy into Eq. 21 provides us

$$\tau_{2R}=0.893\,\tau_{2R}^{\mathrm{IR}}. \tag{28}$$

For slip, $\chi=\infty$ and it follows that

$$\tau_{2R}=0.25\,\tau_{2R}^{\mathrm{IR}}.$$

A χ value of 1.55 is recently reported from the NMR experiment,[26)] and this results in

$$\tau_{2R}=0.799\,\tau_{2R}^{\mathrm{IR}}. \tag{29}$$

Thus a change of 20% in χ causes only a change of 10% in the ratio of τ_{2R} to τ_{2R}^{IR}. The ratio is not so sensitive to χ because f is not a proportional function of χ in Eq. 21.

In Eq. 20, the hydrodynamic boundary conditions (stick or slip) influence τ_{2R}^{IR} as well as f. Comparing Eqs. 1 and 20, on the diffusion level, we have

$$\tau_{2R}=A\frac{\eta}{T}, \tag{30}$$

where

$$A=\frac{1}{4}\left(1+\frac{9}{1+2\chi}\right)A^{\mathrm{IR}}. \tag{31}$$

In the present study, we use Eq. 30 to discuss the effect of solvent and temperature on the NMR rotational correlation time for the C–D bonds of benzene in solution. The experimentally determined hydrodynamic slope A is regarded as a measure reflecting the strength of attractive solute–solvent interactions, as well as the exclusion volume of the solute. The boundary conditions involved in Eq. 30 are assumed to be independent of temperature and pressure.[27)]

Experimental

Materials. Hexane, decane, carbon tetrachloride, chloroform, dichloromethane, methanol, ethanol, 1-propanol, 1-butanol, and acetonitrile were organic solvents of spectro-grade obtained from Nacalai and dried for several days before use by molecular sieves (3A or 4A, Nacalai); they were filtered if necessary. Benzene-d_6 was used as received from CEA. The solutions of benzene-d_6 at 50 mM (M=mol dm^{-3}) were prepared by weight.

Apparatus and Procedure. The ^{2}H spin-lattice relaxation times T_1 for benzene-d_6 were measured with JEOL EX-270WB (wide bore type) spectrometer at 41 MHz. The superconductor magnet bore is wide enough to accommodate a sample tube of 10 mm diameter which is useful for detecting the weak signal of benzene-d_6 at a low concentration of 50 mM. ^{2}H-T_1 was measured by the inversion-recovery method, which has a $[\pi\text{–}t\text{–}\pi/2]_n$ pulse sequence. The largest delay time t was longer than $7T_1$ and the number of delay time n was 20. The free induction decay signals were integrated 2 times. The signal-to-noise ratios were ca. 140. The uncertainty of temperature was ±0.1 °C.

Experimental Results

To clarify the general features of the solvent and temperature effects on the rotational motions of a benzene molecule in solution, we have measured the ^{2}H spin-lattice relaxation times T_1 at 50 mM in various solvents over a wide range of temperature. By means of the measurement over a wide temperature range, from the freezing point to the boiling point, we can discuss the solvent or solvation structure effect on τ_{2R}. The solutions studied are so dilute that solute–solute interactions can be ignored and that the results obtained can be regarded as the limiting values at infinite dilution. The relaxation times measured are converted to the rotational correlation times τ_{2R} through Eq. 14 using the QCC value of 193 kHz along the C–D bond axis.[15)] The rotational motions of benzene in solutions have been explored at rather high concentrations by NMR,[28)] Raman,[29)] and some other methods.[28)] The solvent dependence of the Raman data is in fairly good agreement with that of the present NMR data in view of the differences in concentration and temperature.

In Table 1, the τ_{2R} values for C_6D_6 in C_6D_6 and C_6H_6 are listed for comparison. A small solvent isotope effect on the benzene rotation exists beyond the experimental uncertainties. The rotational correlation time in neat benzene-d_6 is longer by 3—6% than that in normal benzene. The solvent isotope effect can be ascribed to the difference in viscosity between the solvent isotopes; the viscosity of C_6D_6 is reported to be 6.7% larger than that of C_6H_6.[30)] This difference can be ascribed to the difference in the square root of the

Table 1. The Rotational Correlation Times τ_{2R} for C_6D_6 in C_6H_6 and C_6D_6 as a Function of Temperature

	C_6D_6	C_6D_6
	C_6H_6	C_6D_6
T/°C	τ_{2R}/ps	τ_{2R}/ps
5	1.53 ±0.00	1.57 ±0.01
10	1.42 ±0.01	1.51 ±0.01
20	1.28 ±0.01	1.33 ±0.00
30	1.15 ±0.01	1.19 ±0.02
40	1.05 ±0.00	1.09 ±0.01
50	0.973±0.004	1.03 ±0.00
60	0.913±0.012	0.968±0.002
70	0.870±0.000	0.952±0.017

molecular masses or moments of inertia.[31] In contrast to hydrogen bonded liquid water, no decrease of the isotope effect with increasing temperature is observed in non-hydrogen-bonded benzene.

The τ_{2R} values determined in polar and apolar solvents are summarized in Tables 2, 3, and 4. When solvent viscosity is varied with temperature or solvent species, the correlation times increase with increasing solvent viscosity, as predicted by the SED law. The problem is whether the relation is linear and independent of solvent polarity and structure or not.

In Fig. 1, the τ_{2R} values are plotted against solvent viscosities η[32] at 30 °C. If the original SED law like Eq. 1 were valid, the τ_{2R} values would be expected to degenerate into a single straight line because the solute is fixed in this study. On the contrary, the plots generate the three separate lines which are composed of polar, apolar, and alcohol solvent groups. The plots look like a folding fan with three ribs. The largest slope is provided by the aprotic polar solvent group and the smallest by the alcohol homologue. For the hydrocarbon homologue with the medium slope in Fig. 1, the difference in the chain length does not lift up the degeneracy. This is conceivable because solute benzene is solvated by the chain segments which are in vigorous and cooperative motions.

The largest slope can be interpreted in terms of the attractive dipole-induced dipole interactions between the solute

Table 2. The Rotational Correlation Times τ_{2R} for C_6D_6 in Alcohols and Acetonitrile as a Function of Temperature[a)]

	C_6D_6	C_6D_6	C_6D_6	C_6D_6	C_6D_6
	CH_3OH	C_2H_5OH	n-C_3H_7OH	n-C_4H_9OH	CH_3CN
$T/°C$	τ_{2R}/ps	τ_{2R}/ps	τ_{2R}/ps	τ_{2R}/ps	τ_{2R}/ps
−40	2.20	3.02	5.31	7.58	2.21
−30	1.89	2.51	4.07	5.36	1.96
−20	1.60	2.09	3.14	4.00	1.72
−10	1.42	1.79	2.54	3.12	1.50
0	1.30	1.54	2.08	2.50	1.37
10	1.16	1.39	1.79	2.09	1.22
20	1.05	1.25	1.56	1.77	1.15
30	0.978	1.12	1.38	1.55	1.05
40	0.899	1.04	1.20	1.35	0.973
50	0.860	0.952	1.09	1.21	0.950
60	0.841	0.903	1.01	1.09	—
70	—[b)]	0.842	0.938	1.01	—

a) Uncertainties are ±2%. b) Boiling point is 64.7 °C.

Table 3. The Rotational Correlation Times τ_{2R} for C_6D_6 in CH_nCl_{4-n} (n=0,1,2) as a Function of Temperature[a)]

	C_6D_6	C_6D_6	C_6D_6
	CH_2Cl_2	$CHCl_3$	CCl_4
$T/°C$	τ_{2R}/ps	τ_{2R}/ps	τ_{2R}/ps
−40	2.92	4.14	—
−30	2.51	3.48	—[b)]
−20	2.21	2.99	2.55
−10	1.96	2.58	2.21
0	1.76	2.22	1.95
10	1.58	2.00	1.73
20	1.42	1.81	1.56
30	1.30	1.60	1.41
40	—[c)]	1.45	1.28
50	—	1.34	1.20
60	—	1.27	1.14

a) Uncertainties are ±1%. b) Freezing point is −28.6 °C.
c) Boiling point is 40.2 °C.

Table 4. The Rotational Correlation Times τ_{2R} for C_6D_6 in n-C_6H_{14} and n-$C_{10}H_{22}$ as a Function of Temperature[a)]

	C_6D_6	C_6D_6
	n-C_6H_{14}	n-$C_{10}H_{22}$
$T/°C$	τ_{2R}/ps	τ_{2R}/ps
−40	1.75	—[b)]
−30	1.52	3.25
−20	1.36	2.56
−10	1.22	2.11
0	1.11	1.80
10	1.01	1.55
20	0.948	1.38
30	0.853	1.23
40	0.826	1.10
50	0.797	1.01
60	—	0.930
70	—[c)]	0.876
80	—	0.837
90	—	0.772
100	—	0.734

a) Uncertainties are ±1%. b) Freezing point is −29.7 °C.
c) Boiling point is 68.7 °C.

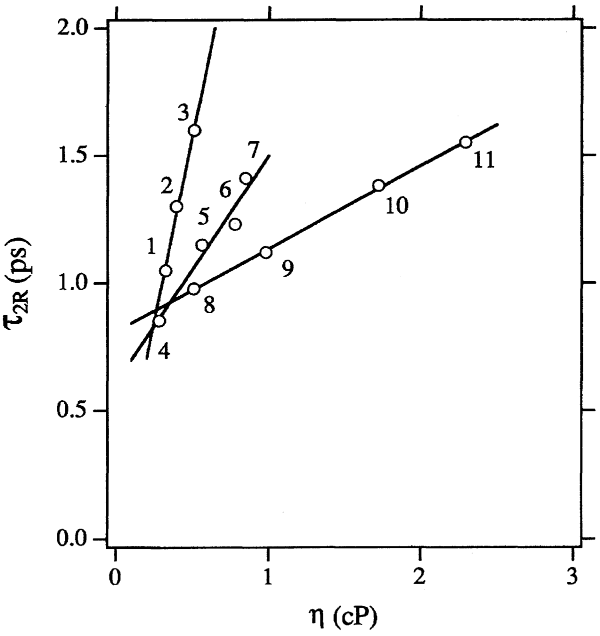

Fig. 1. Plots of the rotational correlation times for C_6D_6 in solutions against solvent viscosities (η in P=0.1 St) at 30 °C. 1, CH_3CN; 2, CH_2Cl_2; 3, $CHCl_3$; 4, n-C_6H_{14}; 5, C_6H_6; 6, n-$C_{10}H_{22}$; 7, CCl_4; 8, CH_3OH; 9, C_2H_5OH; 10, n-C_3H_7OH; 11, n-C_4H_9OH.

and solvent. The smallest slope indicates that the apolar benzene molecule is solvated preferentially by the apolar tail part of the alcohols due to the similarity in the interaction nature. The bulk viscosity of the alcohols is dominated by the hydrogen-bonding interactions between the OH groups, so that the viscosity is much larger than that of the corresponding hydrocarbon. The viscosity shift toward a higher value due to the hydrogen bonds results in a smaller slope of the τ_{2R} vs. η relation, as seen in Fig. 1.

Discussion

Slopes of τ_{2R} vs. η/T Plots. In this section, we focus on the temperature effect on the rotational correlation times for benzene in polar and apolar solvents. In Fig. 2, the τ_{2R} values in CH_nCl_{4-n} (n=0, 1, 2) and some others are plotted against η/T ; η is the solvent viscosity,[32] and T is the temperature. Each plot is linear with a different slope. The slope values summarized in Table 1 are in the order:

$$CHCl_3 > CH_2Cl_2 > CH_3CN > CCl_4 \approx C_6H_6. \qquad (32)$$

This sequence can be understood by considering the polarity and structure of the solvents, i.e., the difference in interactions between solvent–solvent and solute–solvent. Interactions between chloroform molecules are not very strong, as seen from the high volatility and relatively low boiling point, whereas chloroform is a weak proton donor to benzene. The reason why the slope in acetonitrile is smaller than that in dichloromethane, despite the larger molecular dipole moment is that the antiparallel pairing of the highly polar molecules occurs in the liquid structure[33] and that the inert benzene dissolved cannot break the dipolar association. Carbon tetrachloride is as inert as benzene because of the absence of the molecular dipole moment. Such a weak solvation has been found also in the dynamics of solitary water molecules in these apolar solvents. Thus, the slope sequence, Eq. 32, indicates a key role played by attractive solute–solvent and solvent–solvent interactions.

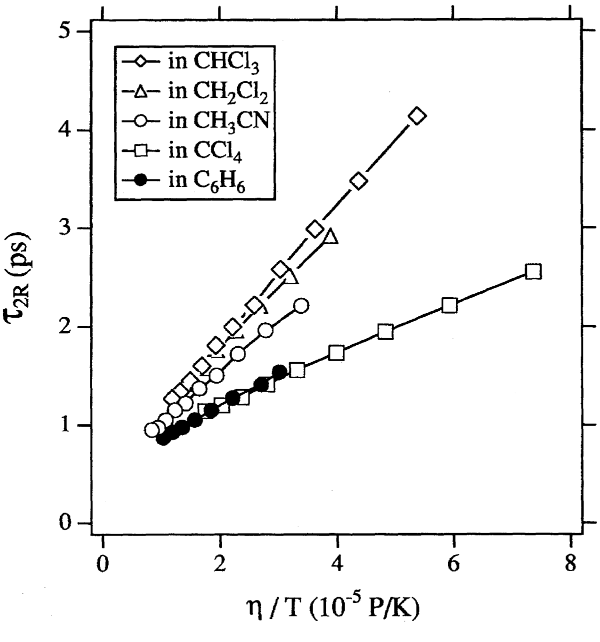

Fig. 2. Plots of the rotational correlation times for C_6D_6 in $CHCl_3$, CH_2Cl_2, CCl_4, CH_3CN, and C_6H_6 against solvent viscosities divided by temperature.

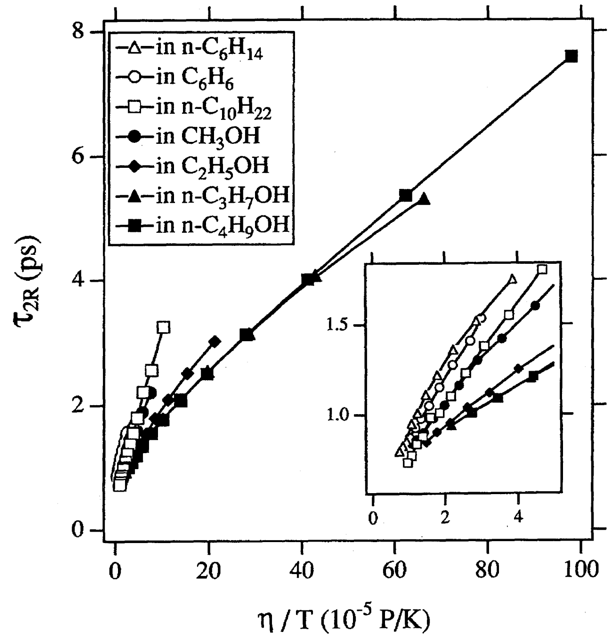

Fig. 3. Plots of the rotational correlation times for C_6D_6 in n-C_6H_{14}, C_6H_6, n-$C_{10}H_{22}$, CH_3OH, C_2H_5OH, n-C_3H_7OH, and n-C_4H_9OH against solvent viscosities divided by temperature. The left bottom portions of the crowded plots are expanded and given as an inset.

As shown in Fig. 3, τ_{2R}–η/T plots are linear in the apolar hydrocarbon solvents, whereas those in such alcohols as methanol, ethanol, 1-propanol, and 1-butanol are concave upward. In the nonlinear case, the slope in the low temperature region is about one half of that in the high temperature (low viscosity) region. The temperature effect observed suggests that the apolar solute molecule prefers the apolar portion of the "amphiphilic" solvent molecule to the polar hydroxyl moiety, in particular at low temperatures. This idea coincides with the conclusion reached above from the solvent effect study. The hydrogen-bonded structure in the alcohols develops more at lower temperatures, so the enhanced hydrogen bonding structure of the solvent alcohols increases their viscosity. However, it provides a much weaker influence on the solute benzene reorientation because of the preferential solvation by the apolar moieties. As a result of the temperature-induced loosening of the hydrogen bonding structure, on the other hand, the probability of finding the interactions between the apolar solute and the polar portion of solvent becomes larger at higher temperatures because of the more random solvent orientations. The longer the alkyl chain of the alcohols, the smaller the hydrodynamic slope. This is reasonable because the increase in the chain length corresponds to a decrease in temperature. It is to be noted that when the viscosity exponent, defined by $\partial \ln \tau_{2R}/\partial \ln \eta$ or $\partial \ln \tau_{2R}/\partial \ln (\eta/T)$, is considered for the viscosity dependence of the rotational correlation times for benzene in the alcohols, the exponent values become considerably smaller than unity (the hydrodynamic value). This must be taken into account in the study of dynamic solvent effect on the reaction dynamics in such "amphiphilic" solvents as alcohols.

The anomalous decrease in the slope with decreasing temperature appears only in the case that the interaction between solute and solvent is *weaker* than that between solvents. In fact, such temperature dependence has been found also for the benzene rotation in the hydrophobic hydration shell in water.[10] The hydrogen-bonded networks are confirmed to be promoted by the presence of the apolar solute benzene, in particular at low temperatures. The decreasing tendency of the slope with decreasing temperature is observed also in the case of hydrophobic hydration in a much narrower range of viscosity; note the two orders of magnitude variation of the viscosity for the alcohols in Fig. 3. The solvent structural effect on the hydrodynamic slope for *benzene* is more remarkable in water which is more strongly hydrogen-bonded than alcohols. The hydrodynamic slope for the NMR rotational correlation time for *water* in the hydrophobic hydration shell of benzene as well as in the bulk *increases* with decreasing temperature as a result of the development of the hydrogen bonds between "solute" and solvent.[10] The contrast between the two cases indicates the importance of the difference or similarity of interactions between solute–solvent and solvent–solvent.

Correlation between Hydrodynamic Slopes and Dissolution Enthalpies. In this section, we examine a correlation between the hydrodynamic slope and the solvation energy. In a previous study, we have found that the solvent effect on the rotational correlation time for solitary waters is correlated with the hydrogen-bonding strength between solute water and organic solvent molecules.[10] As a measure of the thermodynamic solvation energy for a benzene molecule, here we take the dissolution enthalpy at infinite dilution ($\Delta H^{\circ}_{\mathrm{sol}}$). The values of $-\Delta H^{\circ}_{\mathrm{sol}}$ in Table 5 have been computed from the data at finite concentrations.[16] When the benzene–solvent interaction is more attractive than that between benzenes, the dissociation or transfer enthalpy is negative (exothermic); when the former is weaker than the latter, it is positive (endothermic). We test below our view[5,10,15] that the more exothermic the dissolution enthalpy is, the slower will be the molecular rotation in solution.

Table 5. The Slopes A for $\tau_{2\mathrm{R}}$ Plotted against Solvent Viscosities (P=0.1 St) Divided by Temperature and Dissolution Enthalpies $\Delta H^{\circ}_{\mathrm{sol}}$ for C_6H_6 in Solvents

Solvent	A 10^{-7}sKP^{-1}	$-\Delta H^{\circ}_{\mathrm{sol}}$ kJ mol^{-1}
$CHCl_3$	0.69	−1.93
CH_2Cl_2	0.62	−0.09
CH_3CN	0.47	1.21
C_6H_6	0.34	0
n-C_6H_{14}	0.31	3.55
n-$C_{10}H_{22}$	0.27	—
CCl_4	0.25	0.45
CH_3OH	0.22	1.54
C_2H_5OH	0.11	1.63
n-C_3H_7OH	0.057[a)]—0.12[b)]	2.18
n-C_4H_9OH	0.063[a)]—0.12[b)]	2.36

a) Between −40 and −20 °C. b) Between 50 and 70 °C.

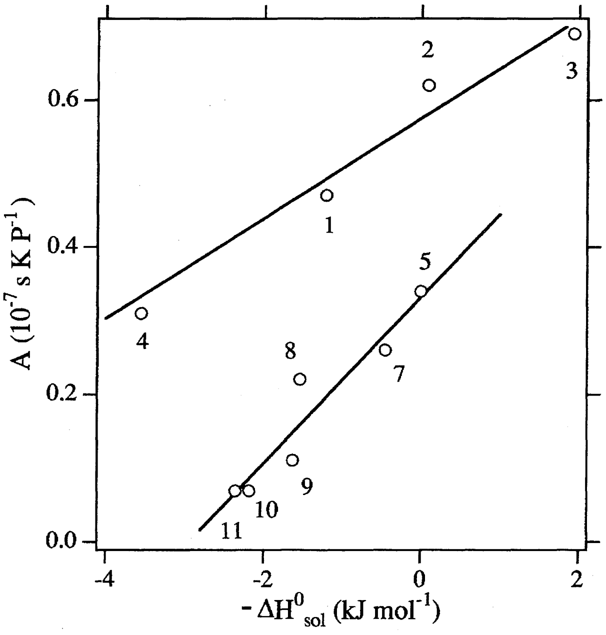

Fig. 4. Plots of the slopes in Figs. 2 and 3 against limiting dissolution enthalpies $\Delta H^{\circ}_{\mathrm{sol}}$ of benzene. The numbers have the same meaning as in Fig. 1.

As seen in Fig. 4, we have positive correlations between A and $-\Delta H^{\circ}_{\mathrm{sol}}$. The correlations are split into the two straight lines with a positive slope. The dissolution enthalpy for benzene in hexane is exceptionally endothermic for some unknown reason. The positive correlations indicate an important role played by attractive intermolecular interaction energies in controlling the rotational correlation times for benzene in solutions. This is in accord with what is observed for solitary waters in organic solvents.[10] Our view reached here on the basis of Eq. 30 is almost equivalent to the alternative consideration of "microviscosity" within the hydrodynamic framework.[17] The present experimental result shows that microscopic theories of molecular rotations in solutions, where solute–solvent interactions are taken into account, need to be developed.

The second author (M. N.) is grateful for the support of this work by the Research Grant-in-Aid No. 07240220 from the Ministry of Education, Science, Sports and Culture. The first author (C. W.) is indebted to JSPS for a Fellowship for the Japanese Junior Scientists.

References

1) G. R. Fleming and P. G. Wolynes, *Phys. Today*, **43**, 36 (1990).

2) D. L. Hasha, T. Eguchi, and J. Jonas, *J. Am. Chem. Soc.*,

104, 2290 (1982).

3) J. Aschcroft, C. L. Xie, and J. Jonas, *J. Chem. Phys.*, **90**, 5386 (1989).

4) C. L. Xie, D. Campbell, and J. Jonas, *J. Chem. Phys.*, **92**, 3736 (1990).

5) M. Nakahara and C. Wakai, *J. Chem. Phys.*, **97**, 4413 (1992).

6) C. Wakai and M. Nakahara, *J. Chem. Phys.*, **100**, 8347 (1994).

7) C. Wakai and M. Nakahara, *J. Chem. Phys.*, **103**, 2025 (1995).

8) M. Nakahara, C. Wakai, and N. Matubayasi, *J. Phys. Chem.*, **99**, 1377 (1995).

9) M. Nakahara and Y. Yoshimoto, *J. Phys. Chem.*, **99**, 10698 (1995).

10) M. Nakahara, C. Wakai, Y. Yoshimoto, and N. Matubayasi, *J. Phys. Chem.*, **100**, 1345 (1996).

11) M. Holtz, R. Haselmeier, R. K. Mazitov, and H. Weingärtner, *J. Am. Chem. Soc.*, **116**, 801 (1994).

12) R. Haselmeier, M. Holtz, W. Marbach, and H. Weingärtner, *J. Phys. Chem.*, **99**, 2243 (1995).

13) M. Nakahara, "Molecular Pictures of Solutions (in Japanese)," ed by the Chemical Society of Japan (H. Ohtaki, M. Nakahara, and H. Nomura), Japan Scientific Societies Press, Tokyo (1995), Chap. 7; S. Ikawa, "Molecular Pictures of Solutions," Chap. 8.

14) C.-Hu and R. Zwanzig, *J. Chem. Phys.*, **60**, 4354 (1974).

15) N. Matsubayashi and M. Nakahara, *J. Chem. Phys.*, **94**, 653 (1991).

16) For benzene in acetonitrile: S. D. Cave, R. D. Santis, and L. Marrelli, *J. Chem. Eng. Data*, **25**, 70 (1980), and for the others; "Kagaku Binran," (Handbook of Chemistry), ed by the Chemical Society of Japan, Maruzen, Tokyo (1993), Part II, Chap. 9.7.

17) a) K. Ibuki and M. Ueno, *Bull. Chem. Soc. Jpn.*, **68**, 1583 (1995); b) K. Ibuki and M. Ueno, *J. Mol. Liquids*, **65/66**, 385 (1995).

18) M. Nakahara and K. Ibuki, *J. Chem. Phys.*, **85**, 4654 (1986).

19) M. Nakahara and K. Emi, *J. Chem. Phys.*, **99**, 5418 (1993).

20) J. Hubbard and L. Onsager, *J. Chem. Phys.*, **67**, 4850 (1977); J. Hubbard, *J. Chem. Phys.*, **68**, 1649 (1978).

21) B. U. Felderhof, *Mol. Phys.*, **48**, 1283 (1983).

22) S. Tang and G. T. Evans, *J. Chem. Phys.*, **103**, 1553 (1995).

23) D. E. Woessner, *J. Chem. Phys.*, **40**, 2341 (1964).

24) J. McConnell, "The Theory of Nuclear Magnetic Relaxation in Liquids," Cambridge University Press, Cambridge (1987).

25) a) W. A. Steele, *Adv. Chem. Phys.*, **34**, 1 (1976); b) F. Perrin, *J. Phys. Radium*, **5**, 497 (1934).

26) a) A. Dölle, M. A. Suhm, and H. Weingärtner, *J. Chem. Phys.*, **94**, 3361 (1991); b) L. Werbelow and A. Thevand, *J. Chem. Phys.*, **96**, 7873 (1992).

27) D. Kivelson and P. A. Madden, *Annu. Rev. Phys. Chem.*, **31**, 523 (1980).

28) D. R. Bauer, G. R. Alms, J. I. Brauman, and R. Pecora, *J. Chem. Phys.*, **61**, 2255 (1974).

29) K. Tanabe and J. Hiraishi, *Mol. Phys.*, **39**, 493 (1980).

30) I. R. Shankland and P. J. Dunlop, *Phys. Rev. B*, **12**, 2249 (1975).

31) H. L. Friedman, in "Molecular Motions in Liquids," ed by J. Lascombe, D. Reidel, Dordrecht (1974), p. 87.

32) a) D. S. Viswanath and G. Natarajan, "Data Book on the Viscosity of Liquids," Hemisphere, New York (1989); b) R. A. Robinson and R. H. Stokes, "Electrolyte Solutions," Butterworths, London (1965), p. 457.

33) H. J. Böhm, I. R. McDonald, and P. A. Madden, *Mol. Phys.*, **49**, 34 (1983).